IMAGING PERFORMANCE OF THE NOBEYAMA MILLIMETER ARRAY

Koh-Ichiro Morita, Masato Ishiguro, Yoshihiro Chikada,
Takashi Kasuga, Ryohei Kawabe, Hideyuki Kobayashi, and Sachiko K. Okumura *
Nobeyama Radio Observatory, National Astronomical Observatory
Nobeyama, Minamimaki, Nagano 384-13, Japan
* Department of Astronomy, University of Tokyo
Hongo, Bunkyo-ku, Tokyo 113, Japan

1. INTRODUCTION

The Nobeyama Millimeter Array (NMA) [1] consists of five 10-m antennas that can be moved to various stations along two baselines of about 500m. The antenna are equipped with SIS receivers [2] developed at the Nobeyama Radio Observatory(NRO) for observations at millimeter wavelengths. The receiver backend is a 320MHz FFT spectro-correlator with 1024 frequency channels per correlation, called as FX [3]. The main purpose of the array is to obtain good quality images at millimeter wavelengths by using the aperture synthesis method [4]. In this wavelength region, however, baseline error and atmospheric fluctuation become large and it is not easy to keep phase stability of the receiver system. These effects degrade the synthesized images. In this paper, we describe the calibration methods and the imaging performance of the NMA.

2. VISIBILITY CALIBRATIONS IN THE NMA

2.1. Model of the observational errors.

The observed complex visibility from an interferometer of two antennas denoted by i and j can be written as,

$$V = G_{ij} V' + \sigma_s \qquad (1)$$

where
V' = True visibility,
G_{ij} = Complex gain of the interferometer,
σ_s = Stochastic complex noise(due to system thermal noise in ideal case).
The complex gain is given as,

$$G_{ij} = b_{ij} a_i \, a_j \qquad (2)$$

where
b_{ij} = baseline based error(due to correlator error, ..),
a_i , a_j = antenna based error(due to baseline error which is relative position error between two antennas, atmospheric phase fluctuation, ..).

2.2. Calibration of baseline errors.

Baseline error is a large component in a_i but time scale of its variation is very slow(~1 month). Therefore we usually calibrate the baseline error just after the reconfiguration of the array. The visibility phase of a point-like radio source whose position is accurately known, consists of phase errors due to the baseline error and the phase offset in the receiver system. If the phase offset is constant during the observation, one can estimate the baseline error from the observations of many point sources. We tried to stabilize LO system in the NMA and improved the method to estimate the baseline errors by use of phase difference between adjascent short observations (5-10min) of many point sources [5]. By these efforts, it became possible to cancel the phase offset and to calibrate the baseline error accurately. Fig.1 is a result of the baseline calibration at 49GHz in November 1988. The residual phase error in

fitting was 3 deg. rms which corresponds to the error of about 70 μm rms.

2.4. Calibration of the bandpass characteristics.

The complex gain is a function of frequency. In the NMA, the amplitude and the phase characteristics across the 1024 frequency channels are calibrated from the 30min observation of strong point sources such as 3C84 or 3C273. The accuracy of the calibration was 6% rms in amplitude and 5 deg. rms in phase.

2.5. Calibration by reference sources.

In the NMA, a 10-15 min observation of a reference calibrator is taken every 30-60 min in order to calibrate the slowly varing complex gain. Since the correlator error of the FX is very small, the complex gain contains only the antenna based error. By this calibration, one can remove the long time scale(30-60min) gain variation from the visibility data.

3. TEST OBSERVATIONS OF THE STRONG POINT SOURCES

We chose 3C84 and 3C273 as test mapping sources, which are the strongest sources at millimeter wavelengths. The observations were made on December 9-10, 1988. We used one of the most compact array configurations in the NMA. The reference calibrator was observed for 15min every 30min. Observational parameters are shown in Table 1. Fig.2 shows an example of the visibility at a baseline of the observation of 3C84.

Center frequency	98GHz	
Total bandwidth	320MHz	
Baseline error	70 μm rms	
Baseline length	20 - 70m	
System noise temparature	200-400K	
Mapping Object	3C84(~20Jy)	3C273(~15Jy)
Bandpass calibrator	3C84	3C273
Reference calibrator	NRA0150(~2Jy)	3C279(~10Jy)
HPBW of synthesized beam	13.5"*6.9"(PA=-79.6deg)	13.3"*9.4"(PA=1.4deg)

Table 1. Observational parameters.

4. RESULTS AND DISCUSSIONS

Fig.3(a) and (b) show the synthesized beam and the map of 3C84, respectively. Large sidelobes in both images are due to the insufficient spatial frequency coverage. It is clear that the synthesized map is very similar to the synthesized beam which is the response to the point source in the case of error free. The peak position of the map differs about 0.6" from the true position. This error is very small(less than 10% of HPBW of the synthesized beam). From Fig.3(b), we subtracted the synthesized beam centered on the peak position of Fig.3(b) and obtained the error map. The peak intensity of subtracted synthesized beam was made equal to that of Fig.3(b). The error map is shown in Fig.3(c). The rms level of Fig.3(c) is 1.5% of the peak intensity of Fig.3(b). These results are summarized in Table 2.

Object	3C84	3C273
Noise(/peak intensity)	1.5%	1.3%
Positional error	(-0.5",-0.6")	(+0.1",+0.5")

Table 2. Errors of the synthesized maps.

The rms baseline error in these observations is 70 μm and corresponding positional error is about 10% of the HPBW. The estimated rms map noise is 0.8%

of the peak intensity. The map noise and the positional error due to the reference calibration error are 0.5% of the peak intensity and <1% of the HPBW, respectively. These estimations are almost consistent with the results of Table 2. The excess of the map noise is probably due to the effect of small time scale atmospheric phase fluctuation.

To obtain the stochastic noise level, σ_s we have applied the SELF-CALIBRATION method [6] to the visibility data. We used a point source model and solved antenna based error in each visibility data. The residuals of this solution might correspond to the stochastic noise level. Fig.4 shows the distribution of the amplitude of the residuals against the spatial frequency. In Fig.4, the stochastic noise level increases as the spatial frequency increases. It means that this stochastic noise of these observations is not only due to the system thermal noise but also due to the effect of short time scale(<30 sec.) atmospheric fluctuations. This effect increases the level of stochastic noise 10 times of that due to the system noise in these observations.

REFERENCES

1. Ishiguro, M. et al. 1984, Proc. of the International Symposium on Millimeter and Submillimeter Wave Radio Astronomy, Granada, reproduced in "Instrumentation and Techniques for Radio Astronomy", ed. Goldsmith, P., IEEE Press, 1988.
2. Kawabe, R. et al. 1989, in preparation.
3. Chikada, Y. et al. 1987, Proceedings of IEEE, 75, 1203.
4. Thompson, A.R., Moran, J.M., and Swenson, G.W., Jr. 1986, "Interferometry and Synthesis in Radio Astronomy", John Wiley & Sons.
5. Morita, K.-I. et al. 1989, in preparation.
6. Schwab, F., 1980, Proc. S.P.I.E., 231, 18.

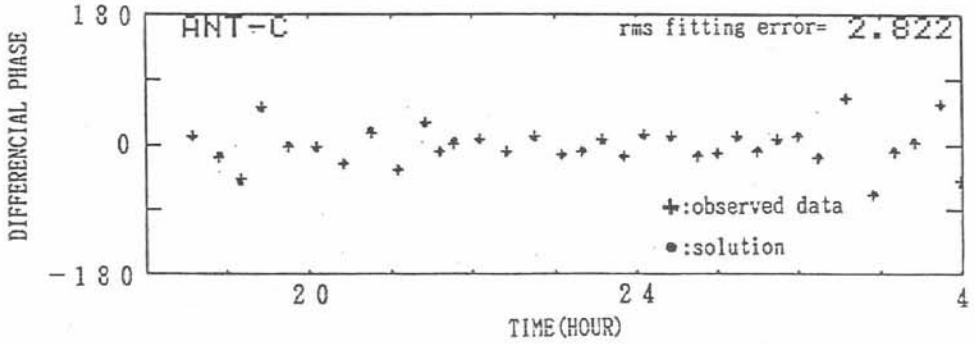

Fig.1. Results of the baseline calibration. Crosses are observed phase differences. Dots are results of the solution.

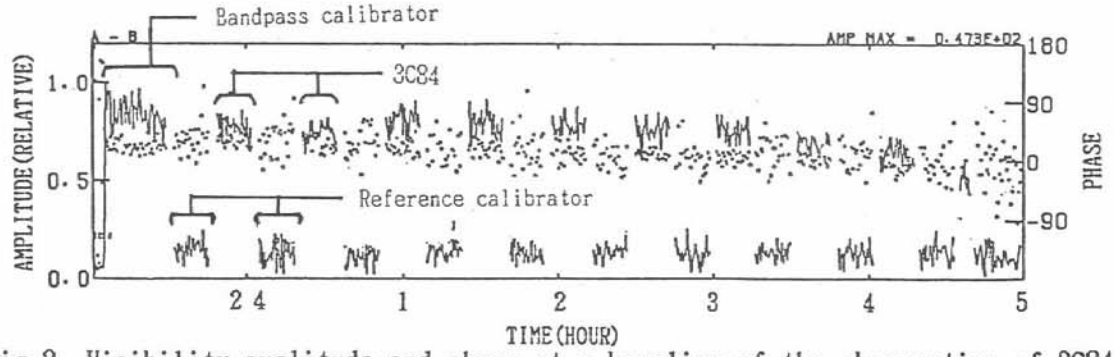

Fig.2. Visibility amplitude and phase at a baseline of the observation of 3C84. Solid lines indicate the amplitude variations and dots indicate the phase variations. This figure also shows the visibility of the bandpass calibrator and the reference calibrator.

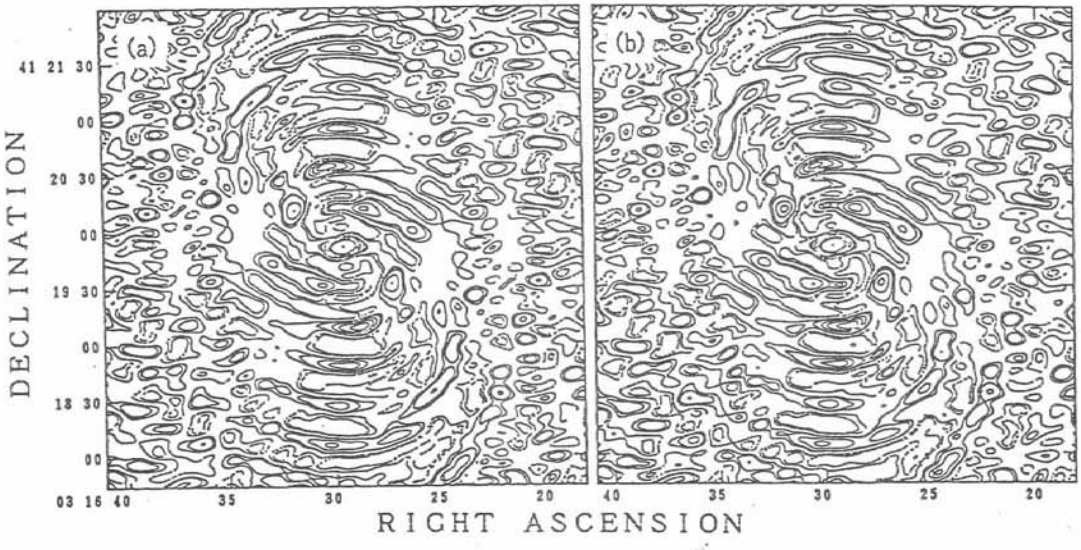

Fig.3(a) Theoretical synthesized beam.
(b) Synthesized map of 3C84.
(c) Error map.
(In (a) and (b), contours are shown for -10,-5,5,10,20,30,40,50,100% of the peak. In (c), contours are shown for -10,-9, · · 8,9,10* (the rms level).)

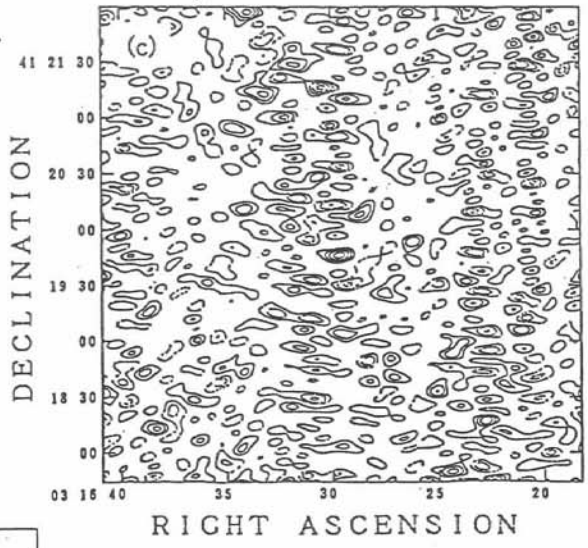

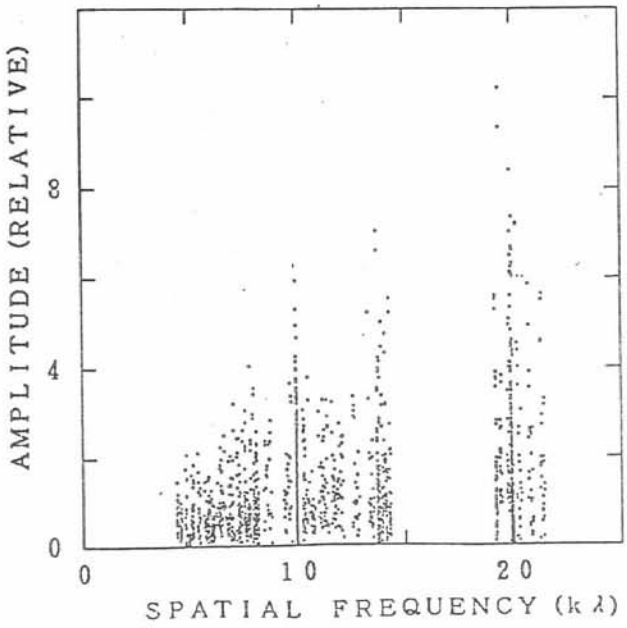

Fig.4. Distribution of the residuals against the spatial frequency after subtracting the point source model with SELF-CALIBRATION.